Carbon nanotube-mediated delivery of nucleic acids does not result in non-specific activation of B lymphocytes

2007 Nanotechnology 18 365101

(http://iopscience.iop.org/0957-4484/18/36/365101)

Nanotechnology **18** (2007) 365101 (10pp) doi:10.1088/0957-4484/18/36/365101

Carbon nanotube-mediated delivery of nucleic acids does not result in non-specific activation of B lymphocytes

Dong Cai[1,4], Cheryl A Doughty[1], Terra B Potocky[1], Fay J Dufort[1], Zhongping Huang[2], Derek Blair[1], Krzysztof Kempa[3], Z F Ren[3] and Thomas C Chiles[1]

[1] Department of Biology, Boston College, Chestnut Hill, MA 02467, USA
[2] NanoLab, Incorporated, Newton, MA 02458, USA
[3] Department of Physics, Boston College, Chestnut Hill, MA 02467, USA

E-mail: caid@bc.edu

Received 12 March 2007, in final form 12 July 2007
Published 10 August 2007
Online at stacks.iop.org/Nano/18/365101

Abstract
The efficient delivery of genes and proteins into primary mammalian cells and tissues has represented a formidable challenge. Recent advances in the research of carbon nanotubes (CNTs) offer much promise for their use as delivery platforms into mammalian cells. Ideally, CNT-mediated applications should not result in cellular toxicity nor perturb cellular homeostasis (e.g., result in non-specific activation of primary cells). It is therefore critical to evaluate the impact of CNT exposure on the cellular metabolism, proliferation and survival of primary mammalian cells. We investigated the compatibility of a recently developed CNT-mediated delivery method, termed nanospearing, with primary *ex vivo* cultures of B lymphocytes. Several parameters were evaluated to assess the impact of CNTs on naïve B lymphocytes, including cell survival, activation, proliferation and intracellular signal transduction. Our results indicate that nanospearing does not result in the activation of naïve primary B lymphocytes nor alter survival in *ex vivo* cultures. Herein, B cells exposed to CNTs were capable of responding to extrinsic pro-survival signals such as interleukin-4 and signaling by the B-cell antigen receptor in a manner similar to that of B cells cultured in the absence of CNTs. Our study demonstrates the biocompatibility of the CNT-mediated nanospearing procedure with respect to primary B lymphocytes.

1. Introduction

The extraordinary properties of carbon nanotubes (CNTs) have stimulated extensive research activities across the world since their discovery in the early 1990s [1]. Various prospective biomedical applications of CNTs have been reported and proposed including biosensing, biointerfacing, molecular delivery and tissue engineering, etc.

In the area of molecule delivery, CNTs with various diameters and length, morphologies, and surface modifications have been used to demonstrate promising molecule introductions into a spectrum of cell types [2–4]. We recently reported the development of a multi-step CNT-mediated delivery platform for plasmid DNA delivery into *ex vivo* mammalian cells and tumor cell lines [5]. The delivery platform, termed nanospearing, relies on CNTs that are synthesized by a plasma enhanced chemical vapor deposition (PECVD) technique. Each CNT contains a Ni particle encapsulated in one end; they are uniform in length, and exhibit a linear morphology. The Ni particle in the presence of an applied magnetic field allows the CNTs to be driven into the cell membrane, thereby delivering into cells the molecule plasmid DNA (coupled to the

[4] Address for correspondence: Biology Department, Boston College, 410 Higgins Hall, Chestnut Hill, MA 02467, USA.

exterior surface of the CNT). We demonstrated efficient delivery of plasmid DNA with accompanying gene expression in difficult-to-transfect primary mammalian cells, including primary cultures of B lymphocytes and neurons [5]. This technique holds promise for the unprecedented efficient delivery of macromolecules into primary cells and tissues, both *in vitro* and *in vivo*. Exposure of mammalian cells to CNTs raises concerns about the biocompatibility, as with other CNT-based delivery methods [2–4, 6]. In order to successfully manipulate the cell function following delivery of macromolecules into mammalian cells by nanospearing, it is critical that exposure to the CNTs and/or the actual spearing process does not perturb the cellular homeostasis (i.e., result in non-specific cellular activation or alter the growth and/or survival responses).

The impact of CNTs on human and animal models has been the subject of numerous investigations with regard to cellular toxicity of the physical and chemical nanotube structure and contaminants resulting from CNT fabrication. Notably, pulmonary toxicity and inflammatory responses have been observed upon intratracheal or intrapharyngeal administration of CNTs [7, 8]. At the cellular level, toxicity has been linked to oxidative stress in both *in vivo* [9, 10] and *in vitro* [11] models. Interestingly, cytotoxicity associated with exposure to single-walled carbon nanotubes (SWNTs) and multi-walled carbon nanotubes (MWNTs) can be minimized by chemical modifications to the nanotube surface [12–15]. Germane to these studies, there is evidence that exposure to and/or uptake of MWNTs induces release of the pro-inflammatory cytokine, interleukin 8, from epithelial keratinocytes [16]. Such cellular and metabolic responses may be cell-type specific insofar as a recent study found that exposure of T cells to CNTs at low dosage (i.e. 40 μg) did not result in altered survival [17], whereas macrophages exposed to an even lower amount of CNTs exhibited cellular necrosis [18]. The same study also showed that SWNTs were more toxic than MWNTs to macrophages [18].

Aberrant growth and survival responses can promote the clonal expansion of B lymphocytes, leading to malignancies and autoimmune diseases. To understand the molecular basis underlying dysregulated B-cell growth and/or survival and ultimately to provide therapeutic intervention, B lymphocytes need to be rendered amenable to the uptake of macromolecules such as recombinant proteins and genes. Nanospearing, the CNT-mediated delivery, allows for the efficient introduction of plasmid DNA into naïve B lymphocytes [5]. It is recognized that the CNTs and the actual spearing process must preserve the naïve 'resting' state of *ex vivo* B cells and result in minimal cytotoxicity. The original procedure of the nanospearing involved multiple steps and, while there was no detectable impact on cell cycle distribution induced by the nanospearing event, we noted by phase contrast microscopy B-cell blasts and cellular aggregation, suggesting non-specific B-cell activation (i.e., increased cell size, activation of signal transduction pathways, increased protein and RNA content, normally associated with stimulation by extrinsic growth factors). We have therefore conducted a comprehensive characterization of the potential effects of exposing *ex vivo* primary B cells to CNTs as it pertains to cellular activation. Our previous method also exploited covalent linkage between plasmid DNA and CNTs. Although DNA immobilization through this avenue has proved effective and has been characterized recently [6, 19], it may reduce the potential to generate stable cell lines with plasmid DNA and preclude effective gene knock-down with siRNA, because these applications require the release of molecules from the CNTs. Herein, we have modified the original multistep nanospearing protocol using a non-covalent DNA immobilization strategy. Furthermore, the compatibility of this delivery method was investigated in *ex vivo* primary B cells with respect to cellular activation, survival, and signal transduction. The results indicate that CNT-mediated nanospearing of primary B cells does not result in non-specific activation of naïve B lymphocytes. We believe that this technique could be used to introduce macromolecules into primary B lymphocytes in order to manipulate cellular signaling, metabolic and growth responses.

2. Experimental details

2.1. Reagents

Poly(L-lysine) (PLL) (70 kD to 140 kD) and 1-ethyl-3-(3-dimethylaminopropyl) carbodiimide (EDC) were purchased from Sigma-Aldrich (Saint Louis, MO). Fluorescein isothiocyanate (FITC) conjugated oligonucleotides (FITC-oligo) (FITC-5′CTTCTTCATGCTCAACCTGGTGCTC3′) in a scrambled sequence (i.e., random sequence that does not correspond to any known mammalian gene) were obtained from Sigma-Genosys (Woodlands, TX). 2.4G2 monoclonal antibody (mAb) was purchased from BD PharMingen (San Diego, CA). $F(ab')_2$ fragments of goat anti-mouse IgM (anti-IgM) were purchased from Jackson ImmunoResearch Laboratories (West Grove, PA). Recombinant mouse interleukin-4 (IL-4) was purchased from BioSource (Camarillo, CA). The anti-phospho (S217/221) MEK1/2 and anti-MEK1/2 antibodies (Abs) were purchased from Cell Signaling Technology (Beverly, MA). Phycoerythrin (PE) conjugated anti-CD71 Ab was obtained from BD Pharmingen (San Diego, CA). All other chemicals were obtained from Sigma-Aldrich.

2.2. B-cell isolation

Balb/c mice were purchased from The Jackson Laboratories (Bar Harbor, ME) and housed at Boston College. The mice were cared for and handled at all times in accordance with the National Institutes of Health and Boston College Institutional Animal Care Use Committee (IACUC) guidelines. Splenic B cells were purified by depletion of T cells with anti-Thy-1.2 plus rabbit complement; macrophages (and other adherent cells) were removed by plastic adherence [20]. Red blood cells and non-viable cells were removed by sedimentation on Lymphocyte-M gradients (Accurate Chemical and Scientific Co., Westbury, MA). The resulting B cells were then centrifuged through discontinuous Percoll gradients in order to isolate quiescent (naïve) B cells [21]. The cells were then cultured in RPMI-1640 medium supplemented with 10 mM HEPES (pH 7.5), 2 mM L-glutamine, 50 μM β-mercaptoethanol, 100 U ml^{-1} penicillin, 100 μg ml^{-1} streptomycin, 0.25 μg ml^{-1} amphotericin B and 10% heat-inactivated fetal calf serum (Atlanta Biologicals, Lawrenceville, GA). B cells were cultured at 3×10^6 cells ml^{-1} in a water-jacketed CO_2 incubator.

2.3. Immunoblotting

Lymphocytes were solubilized in lysis buffer (50 mM Tris-Cl pH 7.4, 150 mM NaCl, 20 mM EDTA, 0.5% Tween-20) containing 1 mM PMSF, 1 mM NaF, 1 mM Na_3VO_4, 10 mM β-glycerophosphate and protease inhibitor cocktail (Sigma-Aldrich). Insoluble debris was removed by centrifugation (10 000 $\times$ g for 10 min, 4 °C). Whole cell lysate protein was separated by polyacrylamide SDS gel electrophoresis and then transferred to Immobilon-P membrane (Millipore, Bedford, MA). Membranes were blocked by incubation in TBS-T (20 mM Tris, pH 7.6, 137 mM NaCl, and 0.05% Tween-20) containing 5% nonfat dry milk for 1 h, followed by incubation overnight with 2 μg ml^{-1} primary Ab. The membrane was then washed with TBS-T, incubated with secondary Ab conjugated horseradish peroxidase (1/2500 dilution) for 1 h, and detected by enhanced chemiluminescence.

2.4. Flow cytometry

B lymphocytes (1–5 $\times$ 10^6 cells) were incubated in 100 μl staining buffer (1 X PBS, 1% FCS, and 0.1% sodium azide) containing 2.4G2 mAb (1:500 dilution) on ice (20 min) to block Fc_γRIIb receptors. Anti-CD71 conjugated PE Ab (1:500 dilution) was then added and incubated for 1 h (4 °C). Parallel B cells were stained with a control isotype conjugated PE antibody. The cells were washed three times with 100 μl of ice-cold staining buffer, resuspended in 500 μl of staining buffer, and analyzed by flow cytometry using a BD FACSCanto flow cytometer (BD Bioscience, San Jose, CA). The data were acquired and analyzed with BD FACSDiva software. To monitor cell viability, B cells were resuspended in 1 ml of staining solution (10 μg ml^{-1} propidium iodide (PI) in 1X PBS) for 5 min and then analyzed by flow cytometry. Bromodeoxyuridine (BrdU) incorporation was carried out according to the manufacturer's instructions (BD Pharmingen). In brief, B lymphocytes were incubated with 20 μM BrdU during the last 24 h of culture. The cells were fixed, permeabilized, and stained with FITC conjugated anti-BrdU Ab (FITC BrdU flow kit). 7-AAD was added to each sample to quantitate DNA content. The cells were analyzed by flow cytometry.

2.5. Microscopy

The cells were absorbed to poly-lysine-coated glass cover slips. The cells were fixed in PBS containing 4% paraformaldehyde for 30 min at room temperature and then stained with 10 ng ml^{-1} PI for 15 min. The cells were then washed twice with ice-cold PBS and analyzed with a Zeiss Axioplan 2 microscope for phase contrast observation and Olympus FluoView FV1000 confocal microscope (Center Valley, PA) section analysis. The three-dimensional reconstruction is based on a stack of 40 sections, and the section depth is 0.3 μm.

2.6. Nanotube preparation

A 2 cm $\times$ 2 cm silicon wafer was coated with chromium and nickel layers of 350 and 30 nm, respectively. The nanotubes were grown in a hot filament PECVD system [5]. A base pressure of 10^{-6} Torr was used before the introduction of acetylene and ammonia gases. The growth pressure was 10–20 Torr, and the growth time was varied between 1 and 10 min. The substrate temperature was maintained below 660 °C. The nanotubes were removed from the silicon wafer and suspended in 5 ml ethyl alcohol at approximately 2 pM. Following centrifugation (10 000 $\times$ g, room temperature) for 10 min, the pellet containing nanotubes was resuspended in 0.5 M HNO_3 to a functionalized CNT with a carboxyl group. The nanotubes were collected by placing a Nd–Fe–B magnet adjacent to the wall of the centrifuge tube (overnight). The nanotubes were then washed three times with deionized water and stored in 5 ml ethyl alcohol at room temperature. The procedure is identical to that previously described [5]. Transmission electron microscopy characterization of the Ni-encapsulated CNT is provided in the supporting information of [5].

2.7. DNA condensation

The PECVD CNTs containing functional carboxyl groups were resuspended in 1 ml 0.1 M 2-[N-morpholino]ethane sulfonic acid (MES) buffer (pH 4.5) containing 10 μl 0.01% PLL and 10 mg EDC to couple the primary amine groups in the PLL molecules to the carboxylic groups on carbon nanotubes. Nanotube PLL complexes (PLL–CNT) were formed after incubation in dark at room temperature for 1 h. The complexes were washed four times with 1 ml MES buffer. The PLL–CNT was incubated with either pBluescript plasmid (pBT) or FITC-oligos. The PLL–CNT nucleic acid complexes (DNA–PLL–CNT) were then condensed [22]. Condensation efficiency was determined by measuring the residual DNA in the extracted supernatant of the condensation mixture by agar gel electrophoresis, ultraviolet–visible spectrometry (DU530, Beckman Coulter, Inc., Fullerton, CA) and fluorescence emission reader (Spectramax plate reader, Molecular Devices, Sunnyvale, CA). The MES buffer was used as the blank. The relative DNA adsorption (%) is calculated according to $100 \times (1 - \frac{\mathrm{Abs}_n}{\mathrm{Abs}_0})\%$, where $\mathrm{Abs}_n = \mathrm{O.D.}^n_{260} - \frac{\mathrm{O.D.}^n_{240} - \mathrm{O.D.}^n_{300}}{2}$, n denotes the index of the samples, and $n = 0$ designates the sample with DNA solution only. Similarly, the supernatant samples of FITC-oligo–PLL–CNT were extracted in the fluorescence measurement.

2.8. Nanospearing

Single-step nanospearing was carried out with Bal17 B-lymphoma cells (3 $\times$ 10^5) or primary murine B lymphocytes (1 $\times$ 10^6) following attachment to PLL-coated cover slips (18 mm diameter). The DNA–PLL–CNTs were resuspended at 2, 0.5, or 0.1 pM in serum-free RPMI-1640 medium. The DNA–PLL–CNT (200 μl) suspension was then applied to each cover slip. The cells were speared by positioning the cover slips directly over a Nd–Fe–B permanent magnet (15 min). The cells were then placed back in the incubator and cultured for 30 min before further assay.

3. Results and discussion

The cell membrane is a formidable barrier to the delivery of therapeutic nucleic acids [23]. A majority of chemical-based artificial DNA delivery systems involve charge neutralization and condensation of DNA into nanometer-scale condensates that facilitate DNA entry into cells [24]. Cationic lipids, for

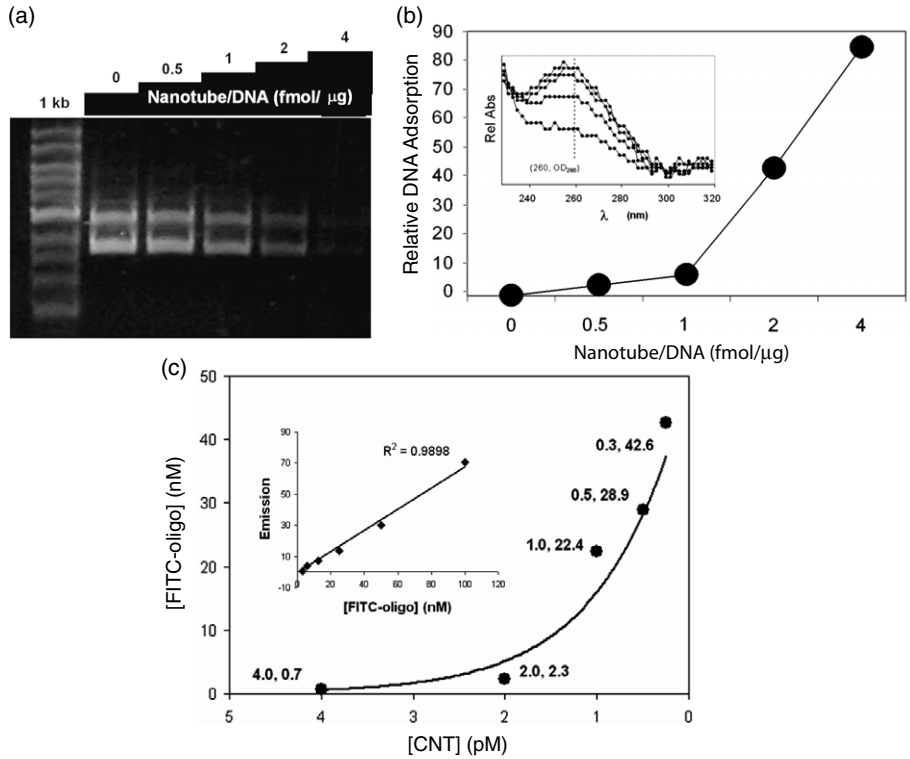

Figure 1. (a) Agarose gel electrophoresis, (b) UV–vis spectrophotometry characterization of plasmid DNA and (c) fluorescence emission measurement of FITC-oligo condensations on PLL–CNTs. The pBT plasmid DNA was mixed with PLL–CNTs at different ratios, i.e. 0, 0.5, 1, 2, and 4 fmol PLL–CNTs per μg DNA. The supernatant was extracted from each sample and loaded to the gel or the spectrometer cuvette in equal volumes. The gel bands and UV absorbance (inset in (b)) represent the remaining DNA in solution, i.e. DNA not complexed to PLL–CNTs. The relative DNA adsorption was calculated as described in section 2. For fluorescence emission measurement, supernatant extractions were collected from FITC-oligo–PLL–CNT assembly mixtures that containing 50 nM FITC-oligo and respectively 4, 2, 1, 0.5 and 0.25 pM PLL–CNTs, of which the FITC-oligo to CNT ratios were 12 500, 25 000, 50 000, 100 000, and 200 000:1 respectively. The inset in (c) is the standard chart of fluorescence emission from FITC-oligo.

example, have enhanced cell transfection by several fold [25]. Efforts to improve oligonucleotide delivery have driven the development of novel reagents for DNA condensation that include cationic liposomes [26, 27], polycationic dendrimers [28], polyethylenimine (PEI) [29, 30] and various cationic peptides [31]. Recently, DNA condensation was also observed on amine functionalized CNTs [32] and polymer grafted CNTs [33]. The toroid- or rod-like condensate DNA structure allows for an enhanced density of DNA loading onto CNTs and a low hydrodynamic radius of the DNA–CNT complex. Moreover, the non-covalent basis of condensation avoids possible DNA mutations, unlike covalent immobilizations, and enables DNA release upon entry into the cells.

We used PLL as a condensation reagent to form the DNA–PLL–CNT complexes between plasmid DNA and functionalized CNTs. As described in section 2, the PLL was first covalently linked to CNTs. DNA was then adhered onto PLL–CNTs via non-covalent electrostatic interactions to form the complete condensation structure. The condensation efficiency of plasmid DNA onto PLL–CNTs was monitored by agarose gel electrophoresis and UV–vis (figure 1). These results suggest that approximately 4 fmol PLL–CNTs is capable of adsorbing greater than 90% of 1 pmol pBluescript plasmid (pBT). Once we had determined the adsorption ability of our CNTs, we employed a 25 mer FITC-oligo to study the CNT-mediated delivery into B cells, and the subsequent effects of the complex on B-cell homeostasis. According to the data in figures 1(a) and (b), each nanotube can carry approximately 250 copies of plasmid DNA (pBT), which is equivalent to 30 000 25 mers. The estimation was confirmed by fluorescence emission measurement of samples from FITC-conjugated oligonucleotide–PLL–CNT complexes (FITC-oligo–PLL–CNTs), as shown in figure 1(c). After FITC-oligo (50 nM) were mixed with PLL–CNTs (2 pM), less than 4 nM FITC-oligo was detected in the supernatant, which means more than 90% of the molecules were absorbed to the PLL–CNTs. To achieve maximum loading of PLL–CNTs with the FITC-oligo 25 mers, the condensation reaction was carried out with 2 fmol nanotubes per μg DNA, (i.e., 60 pmol FITC-oligos).

The compact structure of the DNA–PLL–CNTs resulting from condensation should facilitate plasma membrane penetration, thereby enhancing the plasmid delivery efficiency as well as simplifying the nanospearing procedure. With this in mind, we modified our previously reported multi-step magnetically driven procedure to a single step. Both *ex vivo* primary B lymphocytes and Bal17 B-cell lymphomas were used to demonstrate the efficacy of our single-step nanospearing protocol. The membrane penetration of Bal17 B cells mediated by the nanospearing was evaluated by phase contrast and confocal microscopy as shown in figure 2(a). Visual inspection

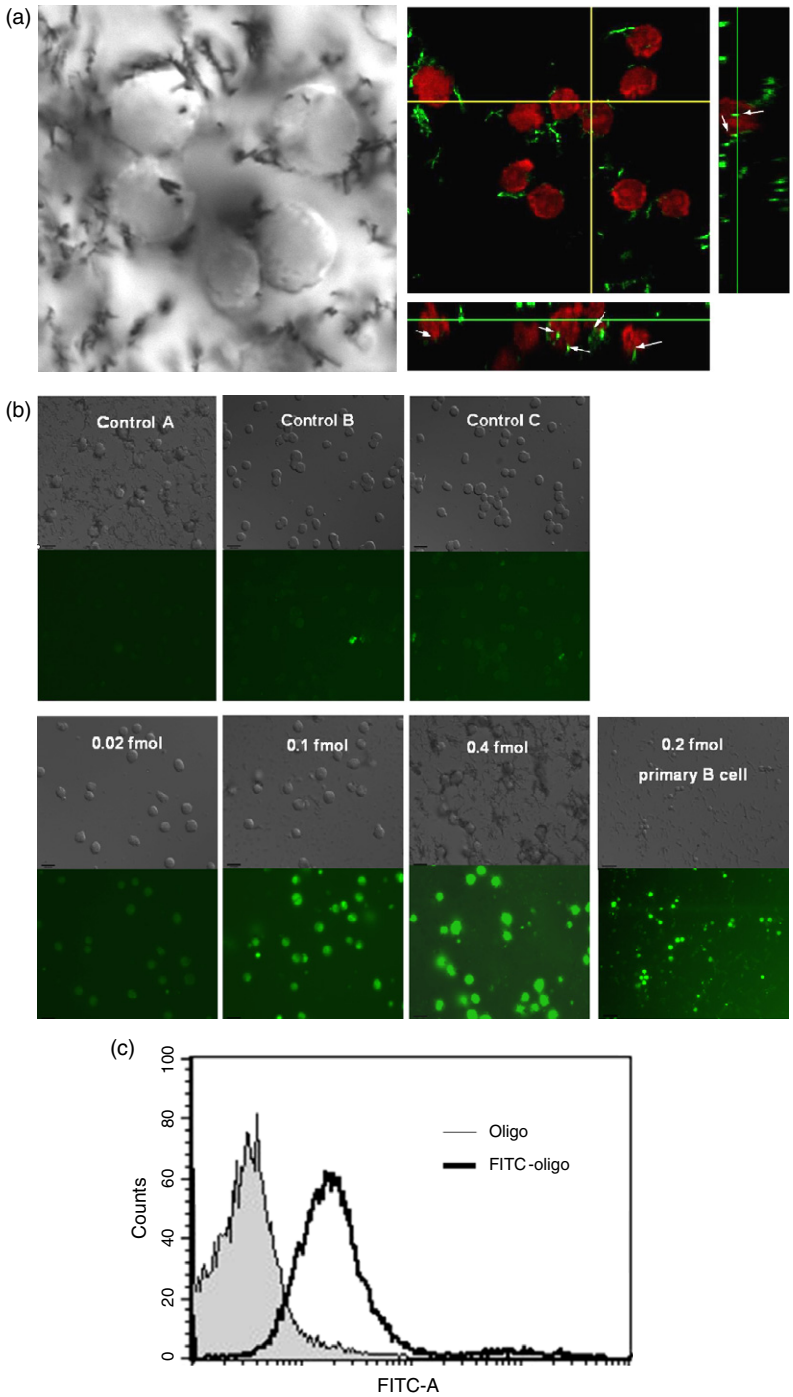

Figure 2. Nanospearing and DNA oligomer delivery. (a) B lymphocytes characterized with phase contrast (left, 30 μm image size) and confocal microscopy (right, 70 μm image size) after being speared by FITC-oligo–PLL–CNTs. Following nanospearing (15 min), the B cells were fixed, stained with PI, and viewed by microscopy with an Olympus FluoView™ FV1000 confocal microscope. A z-series was obtained, consisting of 40 sections, with a total image depth of 12 μm. Captured images are shown as the top view (large image) and vertical-section side views (on the right and bottom sides) of reconstructed 3D images. The top view represents a layer of the sample identified as the green lines in the side-view sections. The yellow lines in the top view mark the positions of sections of each side-view. The white arrows in the side views indicate the locations of CNTs inside the cells. (b) Delivery of FITC-oligo–PLL–CNTs into B lymphocytes following nanospearing. Bal17 cells were speared with 0.4 fmol non-FITC-oligo–PLL–CNT complexes (Control A) or with 0.02, 0.1, or 0.4 fmol FITC-oligo–PLL–CNTs. More control results are shown as 'Control B' (FITC-oligo alone) and 'Control C' (FITC-oligo-PLL) with the corresponding reagent treatments to cell following the spearing procedures. In the lower right panel, primary splenic B cells were nanospeared with 0.2 fmol FITC-oligo–PLL–CNTs. The cells were incubated for 30 min after nanospearing and then examined by confocal microscopy. CNT clusters are noticeable when used at high concentrations, such as in Control, 0.4, and 0.2 fmol. Scale bars = 10 μm. (c) Flow cytometry of B cells following nanospearing. Bal17 cells were subjected to nanospearing with 0.2 fmol FITC-oligo–PLL–CNTs (FITC-oligo) or non-FITC-oligo–PLL–CNTs (oligo, shaded histogram). After 30 min, the cells were analyzed by flow cytometry.

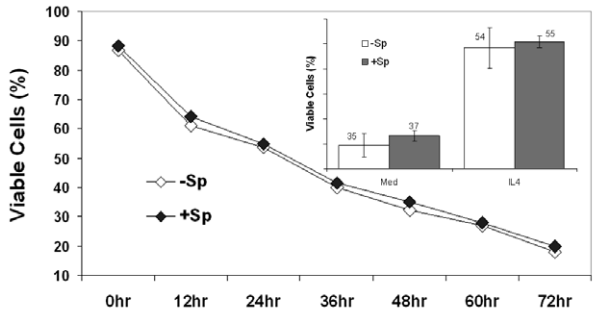

Figure 3. The viability of *ex vivo* B lymphocytes is not affected by nanospearing. B cells were subjected to CNT-mediated nanospearing (+Sp) as described in section 2; control non-nanospeared B cells were cultured in parallel (−Sp). B cells were then cultured in medium. At the indicated times, cells were collected, stained with PI and analyzed by flow cytometry. The inset represents the statistical results of B cells cultured in medium alone (Med) or IL-4 for 48 h ($n = 3$).

reveals both plasma membrane and intracellular localization of FITC-oligo–PLL–CNTs. FITC-oligo–PLL–CNTs were also used to incubate with cells to examine the basal level of CNT internalization. It showed no obvious presence of CNTs inside the cells. Actually, without spearing treatment, the FITC-oligos and cells were not associated well to each other, and most of the CNTs were washed away. This is an unexpected result since it has been widely held that CNTs have the capacity of membrane entry. Since the internalization is a size-sensitive process [34], this result may be ascribed to the relatively large size of the CNTs used here, i.e. 100 nm × 1500 nm (diameter by length) on average. In contrast, the internalized CNTs are either SWNTs or MWNTs between 20 and 30 nm in diameter [2, 3]. Notice that PI can selectively stain the cell nucleus. So the FITC signals inside the PI signal areas in the confocal image indicate nuclear penetration by the FITC-oligo–PLL–CNTs and suggest the ability to modulate intranuclear signaling by nanospearing. Bal17 B cells were also subjected to CNT-mediated nanospearing with varying amounts of FITC-oligo–PLL–CNT complexes. The cells were cultured for 1 h and analyzed by confocal microscopy. As shown in figure 2(b), the intracellular fluorescence signal following delivery increased with the increasing amounts of FITC-oligo–PLL–CNTs. We also achieved efficient delivery of FITC-oligo–PLL–CNT complexes into primary B lymphocytes (figure 2(b), lower right panel). Moreover, flow cytometric analysis of Bal17 cells nanospeared with 0.2 fmol FITC-oligo–PLL–CNT complexes revealed greater than 90% of the B cells expressing a fluorescent signal (figure 2(c)). These results demonstrate efficient delivery of oligonucleotides to B cells via the single-step nanospearing method.

We next sought to evaluate the potential effects of nanospearing on the survival of primary B cells in *ex vivo* culture. It is well established that splenic B lymphocytes die from neglect following culture in the absence of pro-survival cytokines such as IL-4 [35]. B-cell viability was monitored by PI staining and flow cytometry at various times after nanospearing (figure 3). To determine whether nanospearing affected IL-4-dependent survival of splenic B lymphocytes, control and nanospeared B cells were cultured for 48 h in the absence or presence of IL-4. Nanospearing did not affect IL-4-mediated B-cell survival in comparison to control non-nanospeared cells (figure 3, inset).

We next investigated whether nanospearing resulted in a non-specific activation of naïve (resting) *ex vivo* B lymphocytes. Activation of B lymphocytes following cross-linking of the B cell receptor (BCR) with anti-IgM is associated with increased cell size and increased expression of surface markers, such as CD71 and signaling via numerous pathways, including PKC, Akt, and MEK1/2 [36]. Control and nanospeared B cells were stimulated with anti-IgM and then monitored over time for increase in size by flow cytometric forward scatter (FSC). The results suggest that nanospearing does not detectably alter the anti-IgM-mediated increase in cell size beyond that of control B cells (figure 4(a)). The increase in cell size that accompanies stimulation of naïve B cells with IL-4, albeit relatively minor in comparison to anti-IgM, was not affected by nanospearing (figure 4(a)). We also found that culture of nanospeared naïve B cells for 18 h did not result in increased surface CD71 expression in comparison to non-nanospeared B cells (figure 4(b)). In addition, the increase in surface CD71 expression that accompanies cross-linking of the BCR with anti-IgM was not affected by nanospearing (figure 4(b)).

IL-4 treatment of naïve B cells fails to induce proliferation in the absence of a co-stimuli, whereas pre-activation of naïve B lymphocytes renders them responsive to IL-4, as evidenced by G_1-phase progression and DNA replication [37]. Therefore, we sought to determine if nanospearing perturbed naïve splenic B lymphocytes, such that they were rendered competent to proliferate following treatment with IL-4 alone. For these experiments, we used BrdU incorporation to monitor *de novo* DNA synthesis (figure 5). Naïve B cells subjected to nanospearing in the absence of IL-4 did not incorporate BrdU (figure 5, panels marked as 'Unstimulated'). Approximately 5.9% of naïve B lymphocytes treated with IL-4 following nanospearing incorporated BrdU, which was similar to the percentage (5.5%) of non-nanospeared B cells (figure 5, panels marked as 'IL4'), herein suggesting that CNT-mediated nanospearing does not render naïve B cells competent to enter the S phase in response to IL-4. As a control for these studies, BrdU incorporation in B cells stimulated with mitogenic doses of anti-IgM was similar in both control and nanospeared B cells (figure 5, panels marked as 'IgM'), indicating that nanospearing does not affect the ability of mitogenically stimulated B cells to enter the S phase.

Finally, we evaluated whether CNT-mediated nanospearing resulted in the 'non-specific' activation of signaling pathways involved in B-cell proliferation [38]. BCR engagement leads to the activation of MEK1/2 signaling [39]; phosphorylation of MEK1/2 on S217/221 results in catalytic activation [40]. Naïve B cells subjected to nanospearing did not exhibit detectable phosphorylation of MEK1/2 on S217/221, similar to non-nanospeared B cells (figure 6). The phosphorylation of MEK1/2 on S217/221 that accompanies BCR cross-linking with anti-IgM was not affected by nanospearing (figure 6).

We describe herein a modification of a CNT-mediated nanospearing methodology that affords the efficient introduction of oligonucleotides into B lymphocytes in a single step.

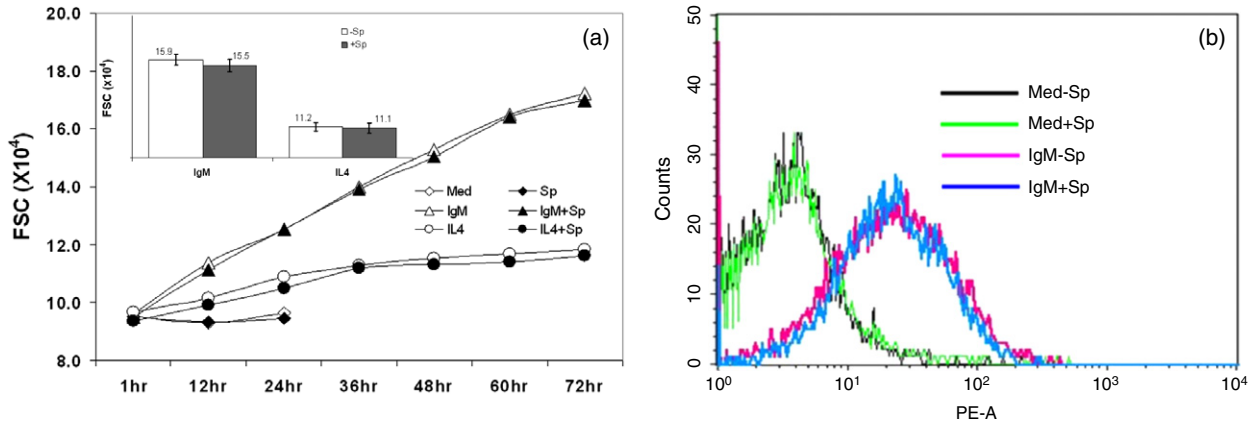

Figure 4. *Ex vivo* B lymphocyte activation after nanospearing characterized by flow cytometry. (a) Increased B-cell size measured by flow cytometry and FSC. B cells were subjected to CNT-mediated nanospearing (+Sp). Control non-nanospeared B cells were cultured in parallel. B cells were then cultured in medium alone (Med), stimulated with 10 μg ml^{-1} anti-IgM (IgM), or 30 ng ml^{-1} IL-4. At the indicated times, cells were collected and analyzed for flow-cytometric FSC. The inset shows the average FSC values at 48 h ($n = 3$). (b) Surface expression of CD71 on naïve and anti-IgM-stimulated B cells after CNT-mediated nanospearing. B cells were subjected to CNT-mediated nanospearing (+Sp); control non-nanospeared B cells were cultured in parallel (-Sp). B cells were then cultured in medium alone (Med) or stimulated with 10 μg ml^{-1} anti-IgM (IgM) for 18 h. The cells were collected and analyzed for CD71 expression by flow cytometry.

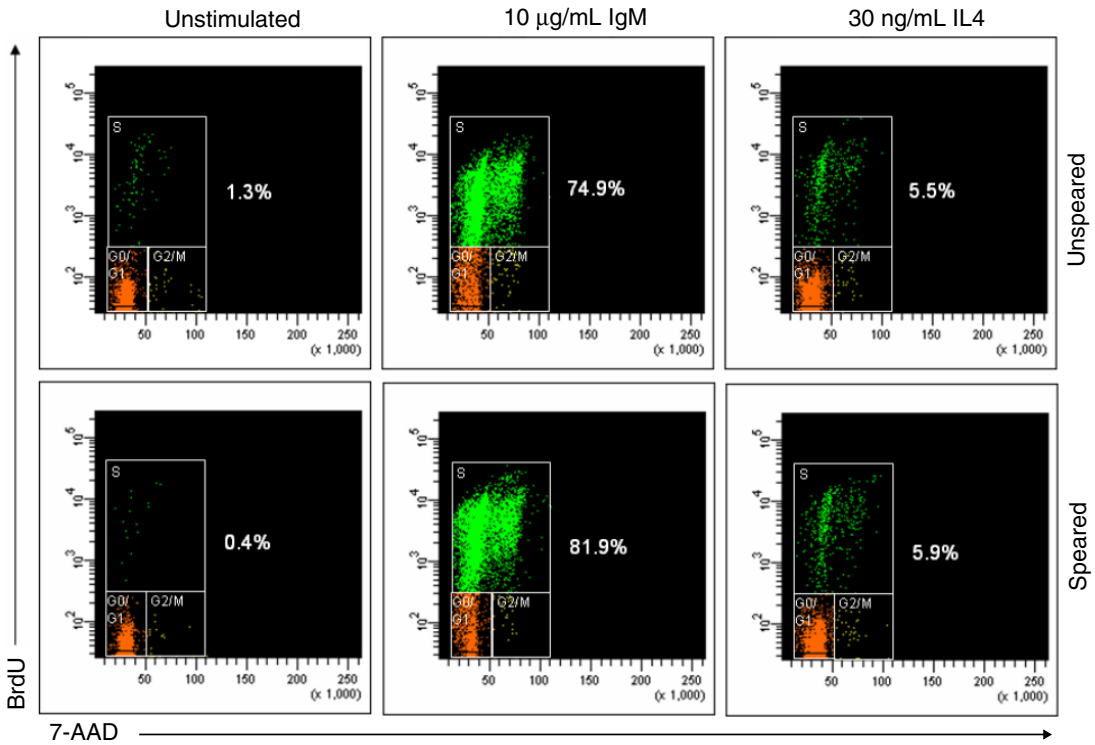

Figure 5. Proliferative responses of primary B lymphocyte following CNT-mediated nanospearing. B cells were subjected to CNT-mediated nanospearing (speared) as described in section 2. Control non-nanospeared B cells were cultured in parallel (unspeared). B cells were then cultured in medium alone (unstimulated), stimulated with 10 μg ml^{-1} anti-IgM, or 30 ng ml^{-1} IL-4 for 48 h. BrdU incorporation was carried out and analyzed by flow cytometry as described in section 2. The cells in the dot plot were gated into three populations that represented cells in the G_0/G_1, G_2/M, and S phase of the cell cycle, respectively. The percentage of cells in the S phase in each condition is show in the panel.

We observe that naïve B cells exposed to CNT-mediated nanospearing in the absence of external stimuli (e.g., IL-4 or anti-IgM) do not exhibit a detectable increase in cell size, surface CD71 expression, or phosphorylation of MEK1/2; we also demonstrate that CNT-mediated nanospearing does not affect the survival of naïve B cells in long-term *ex vivo* cultures. We believe the ability to maintain the 'resting' state of primary B cells may be attributed to the chemical modification of the CNTs (i.e., the functionalization with carboxyl groups and coating with PLL) as well as the low dosage of CNTs used for nanospearing. Indeed, functionalization has been shown to render CNTs less cytotoxic [12–15], even in primary immune cells

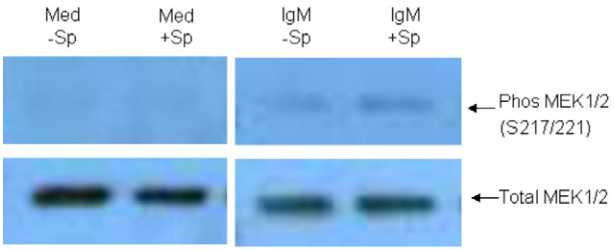

Figure 6. Phosphorylation of MEK1/2 in naïve and anti-IgM stimulated B cells following CNT-mediated nanospearing. B cells were subjected to CNT-mediated nanospearing (+Sp) as described in section 2. Control non-nanospeared B cells were cultured in parallel (−Sp). B cells were then cultured in medium alone (Med) or stimulated with 10 μg ml^{-1} anti-IgM (IgM) for 20 min. The phosphorylation of endogenous MEK1/2 on S217/221 was determined by Western blot analysis (upper panel). The blots were stripped and reprobed for total MEK1/2 protein (lower panel).

(This figure is in colour only in the electronic version)

with SWNTs [41]. We also observed that nanospearing did not induce S-phase entry in naïve B cells subsequently stimulated with IL-4. These findings suggest that the CNTs prepared as outlined herein and/or the actual spearing event do not result in non-specific activation of naïve primary B lymphocytes. Our findings demonstrate that subjecting B cells to nanospearing does not alter their ability to subsequently respond to BCR cross-linking. Although we note some blast-like cells and aggregated cells following nanospearing (by phase contrast microscopy), a plausible explanation could be that the residual magnetism of metal particles in the CNTs tends to generate a magnetic force and cluster the CNT-containing structures together.

The nanospearing technique described here may serve as a platform for the introduction of recombinant proteins, siRNA, and plasmid DNA into primary B cells, without perturbing the 'resting' state. Current methods for the introduction of macromolecules into primary lymphocytes, such as transfection and retroviral-mediated transduction, require prior stimulation with lipopolysaccharide (LPS). In both methods, the transduction efficiency is low (less than 15% of cells) and requires lymphocytes to be engaged in the cell cycle prior to transfection/transduction [42]. These techniques preclude analysis of the cellular and molecular regulation of B-cell activation, proliferation, and cell cycle control. Moreover, these techniques tend to perturb numerous signal transduction pathways and induce the expression of surface activation markers [43]. By contrast, the single-step CNT-mediated spearing procedure described here should allow the introduction of macromolecules into naïve B cells without a prior need to activate or engage B cells in the cell cycle (by stimulation with LPS or the combination of phorbol diester plus calcium ionophore) [44].

It has been previously reported that no appreciable cell death was observed with 10 μg single-wall nanotubes in cultures containing 3×10^5 cells [3]. The amount of CNTs used in our method is only 2 μg,[5] a concentration below the previously determined threshold. Nanospearing, therefore, has the potential for *in vivo* applications where cytotoxicty is a potential concern.

Finally, amine and lysine functionalized CNTs have been shown to exhibit the ability to efficiently condense plasmid DNA [32, 33]. We achieved DNA condensation by covalently linking PLL to CNTs before DNA immobilization. The free amine groups render the complex positively charged, allowing for efficient adsorption of the negatively charged nucleic acid oligomer backbone. Our experiments indicate that DNA condensation onto PLL–CNTs occurs in a similar ratio to that seen for amine functionalized CNTs. Since the condensed plasmid DNA can resist disruptive sonication and DNase I catalyzed hydrolysis [45, 46], we envision that siRNA immobilized by adsorption onto CNTs will remain stable during CNT-mediated delivery.

[5] Concentrate 10 ml CNT suspension in ethyl alcohol by centrifugation and vacuum dry the CNT pellet in a desiccator for 1 day. The weight of CNTs was obtained by measuring with AT261 delta range balance (Mettler-Toledo International Inc., Columbus, OH). Correspondingly, 20 fmol CNTs obtained from 10 ml suspension is about 168 μg.

4. Conclusion

The oligo-PLL–CNT complex formed by the condensation strategy is able to facilitate efficient delivery of nucleic acids into B cells through the single-step nanospearing procedure. Nanospearing does not result in the activation of naïve *ex vivo* primary B cells nor measurably impact subsequent B-cell stimulation via the BCR. These results indicate that CNT-mediated nanospearing can be used to deliver macromolecules into naïve primary B cells in order to study metabolic and proliferative responses.

Acknowledgments

We thank NIBIB of NIH (IR43EB006249) (DC), DOE (DE-FG02-00ER45805) (ZFR) and NSF (NIRT0506830) (ZFR) for supporting the research. Ms Deborah Ritta (Department of Biology, Boston College) has contributed to the research. We thank the Department of Biology for use of the Confocal Microscopy Facility.

References

[1] Iijima S 1991 Helical microtubules of graphitic carbon *Nature* **354** 56

[2] Kostarelos K *et al* 2007 Cellular uptake of functionalized carbon nanotubes is independent of functional group and cell type *Nat. Nanotechnol.* **2** 108

[3] Shi Kam N W, Jessop T C, Wender P A and Dai H 2004 Nanotube molecular transporters: internalization of carbon nanotube–protein conjugates into mammalian cells *J. Am. Chem. Soc.* **126** 6850

[4] Rojas-Chapana J, Troszczynska J, Firkowska I, Morsczeck C and Giersig M 2005 Multi-walled carbon nanotubes for plasmid delivery into *Escherichia coli* cells *Lab Chip* **5** 536

[5] Cai D, Mataraza J M, Qin Z H, Huang Z, Huang J, Chiles T C, Carnahan D, Kempa K and Ren Z 2005 Highly efficient molecular delivery into mammalian cells using carbon nanotube spearing *Nat. Methods* **2** 449

[6] McKnight T E, Melechko A V, Griffin G D, Guillorn M A, Merkulov V I, Serna F, Hensley D K, Doktycz M J, Lowndes D H and Simpson M L 2003 Intracellular integration of synthetic nanostructures with viable cells for controlled biochemical manipulation *Nanotechnology* **14** 551

[7] Lam C W, James J T, McCluskey R, Arepalli S and Hunter R L A 2006 review of carbon nanotube toxicity and assessment of potential occupational and environmental health risks *Crit. Rev. Toxicol.* **36** 189

[8] Muller J, Huaux F, Moreau N, Misson P, Heilier J F, Delos M, Arras M, Fonseca A, Nagy J B and Lison D 2005 Respiratory toxicity of multi-wall carbon nanotubes *Toxicol. Appl. Pharmacol.* **207** 221

[9] Donaldson K, Aitken R, Tran L, Stone V, Duffin R, Forrest G and Alexander A 2006 Carbon nanotubes: a review of their properties in relation to pulmonary toxicology and workplace safety *Toxicol. Sci.* **92** 5

[10] Shvedova A A *et al* 2005 Unusual inflammatory and fibrogenic pulmonary responses to single-walled carbon nanotubes in mice *Am. J. Physiol. Lung Cell Mol. Physiol.* **289** L698

[11] Manna S K, Sarkar S, Barr J, Wise K, Barrera E V, Jejelowo O, Rice-Ficht A C and Ramesh G T 2005 Single-walled carbon nanotube induces oxidative stress and activates nuclear transcription factor—kappaB in human keratinocytes *Nano Lett.* **5** 1676

[12] Sayes C M *et al* 2006 Functionalization density dependence of single-walled carbon nanotubes cytotoxicity *in vitro* *Toxicol. Lett.* **161** 135

[13] Pantarotto D, Singh R, McCarthy D, Erhardt M, Briand J P, Prato M, Kostarelos K and Bianco A 2004 Functionalized carbon nanotubes for plasmid DNA gene delivery *Angew. Chem. Int. Edn Engl.* **43** 5242

[14] Pantarotto D, Briand J P, Prato M and Bianco A 2004 Translocation of bioactive peptides across cell membranes by carbon nanotubes *Chem. Commun.* (1) 16

[15] Singh R, Pantarotto D, Lacerda L, Pastorin G, Klumpp C, Prato M, Bianco A and Kostarelos K 2006 Tissue biodistribution and blood clearance rates of intravenously administered carbon nanotube radiotracers *Proc. Natl Acad. Sci. USA* **103** 3357

[16] Monteiro-Riviere N A, Nemanich R J, Inman A O, Wang Y Y and Riviere J E 2005 Multi-walled carbon nanotube interactions with human epidermal keratinocytes *Toxicol. Lett.* **155** 377

[17] Bottini M, Bruckner S, Nika K, Bottini N, Bellucci S, Magrini A, Bergamaschi A and Mustelin T 2006 Multi-walled carbon nanotubes induce T lymphocyte apoptosis *Toxicol. Lett.* **160** 121

[18] Jia G, Wang H, Yan L, Wang X, Pei R, Yan T, Zhao Y and Guo X 2005 Cytotoxicity of carbon nanomaterials: single-wall nanotube, multi-wall nanotube, and fullerene *Environ. Sci. Technol.* **39** 1378

[19] Mann D G, McKnight T E, Melechko A V, Simpson M L and Sayler G S 2006 Quantitative analysis of immobilized DNA on vertically aligned carbon nanofiber gene delivery arrays *Biotechnol. Bioeng.* **97** 680

[20] Doughty C A, Bleiman B F, Wagner D J, Dufort F J, Mataraza J M, Roberts M F and Chiles T C 2006 Antigen receptor-mediated changes in glucose metabolism in B lymphocytes: role of phosphatidylinositol 3-kinase signaling in the glycolytic control of growth *Blood* **107** 4458

[21] Hodgkin P D, Yamashita L C, Coffman R L and Kehry M R 1990 Separation of events mediating B cell proliferation and Ig production by using T cell membranes and lymphokines *J. Immunol.* **145** 2025

[22] Zauner W, Ogris M and Wagner E 1998 Polylysine-based transfection systems utilizing receptor-mediated delivery *Adv. Drug Delivery Rev.* **30** 97

[23] Zabner J, Fasbender A J, Moninger T, Poellinger K A and Welsh M J 1995 Cellular and molecular barriers to gene transfer by a cationic lipid *J. Biol. Chem.* **270** 18997

[24] Mahato R I, Takakura Y and Hashida M 1997 Nonviral vectors for *in vivo* gene delivery: physicochemical and pharmacokinetic considerations *Crit. Rev. Ther. Drug Carr. Syst.* **14** 133

[25] Gao X and Huang L 1996 Potentiation of cationic liposome-mediated gene delivery by polycations *Biochemistry* **35** 1027

[26] Capaccioli S, Dipasquale G, Mini E, Mazzei T and Quattrone A 1993 Cationic lipids improve antisense oligonucleotide uptake and prevent degradation in cultured cells and in human serum *Biochem. Biophys. Res. Commun.* **197** 818

[27] Lewis J G, Lin K Y, Kothavale A, Flanagan W M, Matteucci M D, DePrince R B, Mook R A, Hendren R W and Wagner R W 1996 A serum-resistant cytofectin for cellular delivery of antisense oligodeoxynucleotides and plasmid DNA *Proc. Natl Acad. Sci. USA* **93** 3176

[28] Yoo H and Juliano R L 2000 Enhanced delivery of antisense oligonucleotides with fluorophore-conjugated PAMAM dendrimers *Nucleic Acids Res.* **28** 4225

[29] Boussif O, Lezoualch F, Zanta M A, Mergny M D, Scherman D, Demeneix B and Behr J P 1995 A versatile vector for gene and oligonucleotide transfer into cells in culture and *in vivo*: polyethylenimine *Proc. Natl Acad. Sci. USA* **92** 7297

[30] Robaczewska M *et al* 2001 Inhibition of hepadnaviral replication by polyethylenimine-based intravenous delivery of antisense phosphodiester oligodeoxynucleotides to the liver *Gene Ther.* **8** 874

[31] Lochmann D, Jauk E and Zimmer A 2004 Drug delivery of oligonucleotides by peptides *Eur. J. Pharm. Biopharm.* **58** 237

[32] Singh R, Pantarotto D, McCarthy D, Chaloin O, Hoebeke J, Partidos C D, Briand J P, Prato M, Bianco A and Kostarelos K 2005 Binding and condensation of plasmid DNA onto functionalized carbon nanotubes: toward the construction of nanotube-based gene delivery vectors *J. Am. Chem. Soc.* **127** 4388

[33] Liu Y, Wu D C, Zhang W D, Jiang X, He C B, Chung T S, Goh S H and Leong K W 2005 Polyethylenimine-grafted multiwalled carbon nanotubes for secure noncovalent immobilization and efficient delivery of DNA *Angew. Chem. Int. Edn Engl.* **44** 4782

[34] Gao H, Shi W and Freund L B 2005 From the cover: mechanics of receptor-mediated endocytosis *Proc. Natl Acad. Sci. USA* **102** 9469

[35] Broxmeyer H E, Lu L, Cooper S, Tushinski R, Mochizuki D, Rubin B Y, Gillis S and Williams D E 1988 Synergistic effects of purified recombinant human and murine B cell growth factor—1/IL-4 on colony formation *in vitro* by hematopoietic progenitor cells *J. Immunol.* **141** 3852

[36] Lok C N and Loh T T 1998 Regulation of transferrin function and expression: review and update *Biol. Signals Recept.* **7** 157

[37] Oliver K, Noelle R J, Uhr J W, Krammer P H and Vitetta E S 1985 B-cell growth factor (B-cell growth factor I or B-cell-stimulating factor, provisional 1) is a differentiation factor for resting B cells and may not induce cell growth *Proc. Natl Acad. Sci. USA* **82** 2465

[38] Gold M R 2002 To make antibodies or not: signaling by the B-cell antigen receptor *Trends Pharmacol. Sci.* **23** 316

[39] Chang F, Steelman L S, Lee J T, Shelton J G, Navolanic P M, Blalock W L, Franklin R A and McCubrey J A 2003 Signal transduction mediated by the Ras/Raf/MEK/ERK pathway from cytokine receptors to transcription factors: potential targeting for therapeutic intervention *Leukemia* **17** 1263

[40] Jazirehi A R, Vega M I, Chatterjee D, Goodglick L and Bonavida B 2004 Inhibition of the Raf-MEK1/2-ERK1/2 signaling pathway, Bcl-xL down-regulation, and chemosensitization of non-Hodgkin's lymphoma B cells by Rituximab *Cancer Res.* **64** 7117

[41] Dumortier H, Lacotte S, Pastorin G, Marega R, Wu W, Bonifazi D, Briand JP, Prato M, Muller S and Bianco A 2006 Functionalized carbon nanotubes are non-cytotoxic and preserve the functionality of primary immune cells *Nano Lett.* **6** 1522

[42] Wilcox H M and Berg L J 2003 Itk phosphorylation sites are required for functional activity in primary T cells *J. Biol. Chem.* **278** 37112

[43] McMahon S B, Norvell A, Levine K J and Monroe J G 1995 Transient transfection of murine B lymphocyte blasts as a

method for examining gene regulation in primary B cells *J. Immunol. Methods* **179** 251

[44] DeFranco A L, Raveche E S and Paul W E 1985 Separate control of B lymphocyte early activation and proliferation in response to anti-IgM antibodies *J. Immunol.* **135** 87

[45] Kogurea K, Moriguchib R, Sasakib K, Uenoc M, Futakid S and Harashima H 2004 Development of a non-viral multifunctional envelope-type nano device by a novel lipid film hydration method *J. Control. Release* **98** 317

[46] Abdelhady H G, Allen S, Davies M C, Roberts C J, Tendler S J B and Williams P M 2003 Direct real-time molecular scale visualisation of the degradation of condensed DNA complexes exposed to DNase I *Nucleic Acids Res.* **31** 4001